Experimental and theoretical demonstration of validity and limitations in fringe-resolved autocorrelation measurements for pulses of few optical cycles

K. Yamane, T. Kito, R. Morita, and M. Yamashita

Department of Applied Physics, Faculty of Engineering, Hokkaido University, Kita-13, Nishi-8, Kita-ku, Sapporo, 060-8628 Japan

k-yamane@eng.hokudai.ac.jp

Abstract: Using 3.6- and 5.3-fs pulses, we demonstrated theoretically and experimentally that fringe-resolved autocorrelation (FRAC) traces are distorted by bandwidth limitations of the second-harmonic generation (SHG) in 10-μm-thick, type I β-BaB_2O_4 for pulses shorter than sub-5 fs. In addition, detailed numerical analysis of the SHG showed that the optimum crystal angle where the FRAC trace distortion becomes minimum is in disagreement not only with the phase-matching angle but also with the angle where the FRAC signal intensity becomes maximum. Furthermore, the apparent pulse duration measured at a nonoptimum angle was confirmed to become shorter than that of its transform-limited pulse, in excellent agreement with the calculated result.

OCIS codes: (320.5520) Ultrafast measurements; (320.7100) Pulse compression.

References and links

1. J.-C. M. Diels, J. J. Fontaine, I. C. McMichael, and F. Simoni, "Control and measurement of ultrashort pulse shapes (in amplietude and phase) with femtosecond accuracy," Appl. Opt. **24**, 1270 (1985).
2. N. Karasawa, L. Li, A. Suguro, H. Shigekawa, R. Morita, and M. Yamashita,"Optical pulse compression to 5.0 fs by use of only a spatial light modulator for phase compensation," J. Opt. Soc. Am. B **18**, 1742 (2001).
3. A. Cheng, G. Tempea, T. Brabec, K. Ferencz, and F. Krausz, "Generation of intense diffraction-limited white light and 4-fs pulses," in *Ultrafast Phenomena XI* (Springer-Verlag, Berlin, 1998), p. 8.
4. Z. Cheng, A. Fürbach, S. Sartania, M. Lenzner, Ch. Spielmann, and F. Krausz, "Amplitude and chirp characterization of high-power laser pulses in the 5-fs regime," Opt. Lett. **24**, 247 (1999).
5. A. Shirakawa, I. Sakane, M. Takasaka, and T. Kobayashi, "Sub-5-fs visible pulse generation by pulse-front-matched non-collinear optical parametric amplification," Appl. Phys. Lett. **74**, 2268 (1999).
6. A. Baltuška, M. S. Pshenichnikov, and D. A. Wiersma, "Second-harmonic generation frequency-resolved optical gating in the single-cycle regime," IEEE J. Quantum Electron. **35**, 459 (1999).
7. M. Hirasawa, N. Nakagawa, K. Yamamoto, R. Morita, H. Shigekawa, M. Yamashita, "Sensitivity improvement of spectral phase interferometry for direct electric-field reconstruction for the characterization of low-intensity femtosecond pulses," Appl. Phys. B **74**, S225-229 (2002).
8. K. Yamane, Z. Zhang, K. Oka, R. Morita, M. Yamashita, and A. Suguro, "Optical pulse compression to 3.4 fs in the monocycle region by feedback phase compensation," Opt. Lett. **28**, 2258 (2003).
9. A. M. Weiner, "Effect of group velocity mismatch on the measurement of ultrashort optical pulses via second harmonic generation," IEEE J. Quantum Electron. **19**, 1276 (1983).
10. Ch. Spielmann, L. Xu, and F. Krausz, "Measurement of interferometric autocorrelations: comment," Appl. Opt. **36**, 2523 (1997).

#4106 - $15.00 US Received 26 March 2004; revised 14 May 2004; accepted 6 June 2004

11. R. Morita, M. Hirasawa, N. Karasawa, S. Kusaka, N. Nakagawa, K. Yamane, L. Li, A. Suguro, and M. Yamashita, "Sub-5 fs optical pulse characterization," Meas. Sci. Technol. **13**, 1710-1720 (2002).
12. V. G. Dmitriev, G. G. Gurzadyan, and D. N. Nikogosyan, *Handbook of Nonlinear Optical Crystals* (Springer-Verlag, Berlin, 1991).

1. Introduction

A fringe-resolved autocorrelation (FRAC) method [1] with second-harmonic (SH) generation is widely used for the measurement of ultrashort optical pulses even with durations shorter than 10 fs because of its simplicity. However, this method has several problems. First, it is difficult to measure pulses with spectra of more than one octave because a bandpass filter is needed to separate the SH signal from fundamental pulses to be measured and hence distorts its SH signal. Second, the method requires the assumption of a pulse shape, for example, Gaussian, sech^2. This ambiguity causes a determinate error of the measured pulse duration. The former problem is difficult to solve in principle, but the latter may be avoided by comparing a measured FRAC trace with a calculated trace by use of its spectrum. Nevertheless, the measured pulse duration tends to be evaluated to be shorter [2, 3, 4, 5] than that obtained by other measurement methods, for example, frequency-resolved optical gating (FROG) [2, 4, 6] and spectral phase interferometry for direct electric-field reconstruction (SPIDER) [7, 8, 11]. In addition, the measured pulse duration is sometimes evaluated to be shorter than that of its Fourier–transform-limited (TL) pulses. However, the origin of these kinds of problems and quantitative limitation of the FRAC method have not, to our knowledge, been closely scrutinized, except in Refs. [9] and [10]. In the former [9], the effect of group-velocity mismatch on the intensity autocorrelation method was discussed. On the other hand, in the latter [10], the influence of the asymmetric Michelson interferometer in FRAC measurement for sub-10-fs pulses was identified.

In this paper, we investigate the influence of the frequency-dependent efficiency of the SH generation of few-cycle pulses to be measured by the FRAC method as the main origin. For ultrabroadband optical pulses, we cannot consider that the SH electric field generated even in a thin nonlinear crystal is proportional to the square of the incident temporal electric field because of the limitation of phase-matching bandwidth in the SH generation. We verify theoretically and experimentally such a bandwidth-limitation effect in FRAC measurement with type I, 10-μm thick β-BaB_2O_4 (BBO), using two optical pulses of 5.3 and 3.6 fs. Furthermore, we demonstrate that the boundary pulse duration between the validity and the limitation of the FRAC method is in the sub-5-fs range.

2. Equations for FRAC signals

FRAC signal is obtained by measuring the intensity of the SH wave generated from an incident pulse pair with a relative delay time τ as a function of its τ by use of a "slow" detector. The ideal signal $S_{\mathrm{FRAC}}(\tau)$ is expressed by the following well-known form [1]:

$$S_{\mathrm{FRAC}}(\tau) = 2G(0) + 4G(\tau) + 4\mathrm{Re}\left[F_1(\tau)\right] + 2\mathrm{Re}\left[F_2(\tau)\right], \tag{1}$$

where

$$\begin{aligned} G(\tau) &= \int_{-\infty}^{\infty} \left|E(t)\right|^2 \left|E(t-\tau)\right|^2 \mathrm{d}t, \\ F_1(\tau) &= \int_{-\infty}^{\infty} \left[E(t)^2 + E(t-\tau)^2\right] E^*(t) E^*(t-\tau) \mathrm{d}t, \\ F_2(\tau) &= \int_{-\infty}^{\infty} E^2(t) E^{*2}(t-\tau) \mathrm{d}t, \end{aligned} \tag{2}$$

#4106 - $15.00 US Received 26 March 2004; revised 14 May 2004; accepted 6 June 2004

and the linearly polarized electric field $E(t)$ of the positive frequency ω component in a complex representation is expressed by the real electric field $\varepsilon(t)$ including a carrier-wave term with a time-dependent phase $\varphi(t)$, as follows:

$$E(t) = \int_0^\infty \tilde{\varepsilon}(\omega)\exp[-\mathrm{i}\omega t]\mathrm{d}\omega, \;\; \tilde{\varepsilon}(\omega) = \int_{-\infty}^\infty \varepsilon(t)\exp[\mathrm{i}\omega t]\mathrm{d}t. \tag{3}$$

However, the SH generation is limited by a phase-matching bandwidth in a nonlinear crystal. Especially, for few-optical-cycle pulses, the investigation of the bandwidth limitation effect is indispensable. Here, for the sake of simplicity, let us consider the frequency-dependent efficiency of the SH generation from a thin nonlinear crystal in the frequency domain.

The SH electric field generated from a nonlinear crystal is derived from a nonlinear propagation equation [6]. The intensity $I_{\mathrm{SH}}(\Omega,\tau)$ of the SH electric field at an SH frequency Ω and a delay time τ with respect to a uniaxial negative nonlinear crystal such as BBO is given by

$$\begin{aligned} I_{\mathrm{SH}}(\Omega,\tau) &\propto \frac{\Omega}{n_e(\Omega)}\Big|\int_{-\infty}^\infty \sqrt{\omega(\Omega-\omega)}\exp[\mathrm{i}V(\Omega,\omega)L]\mathrm{sinc}[V(\Omega,\omega)L] \\ &\quad \times[n_{\mathrm{e}}^2(\Omega)-1][n_{\mathrm{o}}^2(\Omega-\omega)-1](n_{\mathrm{o}}^2(\omega)-1) \\ &\quad \times\tilde{E}(\omega)\tilde{E}(\Omega-\omega)(1+\exp[\mathrm{i}\omega\tau])\{1+\exp[\mathrm{i}(\Omega-\omega)\tau]\}\mathrm{d}\omega\Big|^2 \\ &\equiv I_{\mathrm{SH,no\_SFA}}(\Omega,\tau) \end{aligned} \tag{4}$$

(SFA in the subscript is the shortened representation of spectral filter approximation, which is mentioned in the next paragraph) with a quantity concerning the type I phase-matching condition

$$V(\omega,\Omega-\omega) = \frac{k_{\mathrm{o}}(\omega)+k_{\mathrm{o}}(\Omega-\omega)-k_{\mathrm{e}}(\Omega)}{2}, \tag{5}$$

where $n_{\mathrm{o}}(\omega)$ and $n_{\mathrm{e}}(\omega)$ are linear refractive indices for ordinary and extraordinary beams, respectively; $k_{\mathrm{o}}(\omega)$ and $k_{\mathrm{e}}(\omega)$ are wave numbers for ordinary and extraordinary beams, respectively; L is the crystal length; and $\tilde{E}(\omega)$ is the Fourier transform of the incident pulse electric field $E(t)$. We have assumed that the beam diameter depends on the frequency and is proportional to $1/\sqrt{\omega}$ as Eq. (9) in Ref. [6] (It is experimentally confirmed that the beam diameter has such dependence for our hollow fiber, although it is thought that the beam waist has no frequency dependence for a hollow fiber as pointed out in Ref. [6]). In addition, we approximated the second order susceptibility $\chi^{<2>}(\Omega,\omega,\Omega-\omega)$ by the product of the linear susceptibility $\chi^{<1>}(\omega)=\chi(n^2(\omega)-1)$, that is, $\chi^{<2>}(\Omega,\omega,\Omega-\omega)\propto\chi(n_{\mathrm{e}}^2(\Omega)-1)(n_{\mathrm{o}}^2(\omega)-1)(n_{\mathrm{o}}^2(\Omega-\omega)-1)$.

Under approximations $[\omega(1-\omega/\Omega)]^{1/2}\simeq\sqrt{\Omega}/2$ and $V(\omega,\Omega-\omega)\simeq V(\Omega/2,\Omega/2)$ (we expanded $k_{\mathrm{o}}(\omega)$ and $k_{\mathrm{o}}(\Omega-\omega)$ into the Taylor series around $\Omega/2$ up to the first order) in Eq. (4) [6], the intensity of the SH field can be conveniently decomposed to a product of a spectral filter function $R(\Omega)$ and an ideal SH intensity $I_{\mathrm{SH,ideal}}(\Omega,\tau)$ without taking account of the influence of the bandwidth limitation resulting from the SH wave conversion, as follows [the $I_{\mathrm{SH,no\_SFA}}(\Omega,\tau)$ of Eq. (4) is the equation without those approximations]:

$$I_{\mathrm{SH,no\_SFA}}(\Omega,\tau) \simeq R(\Omega)I_{\mathrm{SH,ideal}}(\Omega,\tau) \equiv I_{\mathrm{SH,with\_SFA}}(\Omega,\tau), \tag{6}$$

where

$$R(\Omega) = \frac{\Omega^3}{4n_e(\Omega)}\left[\left(n_{\mathrm{e}}^2(\omega)-1\right)\left(n_{\mathrm{o}}^2(\Omega/2)-1\right)^2\mathrm{sinc}[V(\Omega/2,\Omega/2)L]\right]^2, \tag{7}$$

$$I_{\mathrm{SH,ideal}}(\Omega,\tau) = \left|\int_{-\infty}^\infty \tilde{E}(\omega)\tilde{E}(\Omega-\omega)(1+\exp[\mathrm{i}\omega\tau])(1+\exp[\mathrm{i}(\Omega-\omega)\tau])\mathrm{d}\omega\right|^2. \tag{8}$$

#4106 - $15.00 US
Received 26 March 2004; revised 14 May 2004; accepted 6 June 2004

We will call the decomposition "spectral filter approximation."

Three different signals $S_{\mathrm{SH},\alpha}(\tau)$s are obtained by integrating $I_{\mathrm{SH},\alpha}(\Omega,\tau)$s over the whole spectral range (α = no_SFA, with_SFA and ideal):

$$S_{\mathrm{SH},\alpha}(\tau) \quad = \quad \int_{-\infty}^{\infty} I_{\mathrm{SH},\alpha}(\Omega,\tau)\,\mathrm{d}\Omega \;\; (\alpha = \text{no\_SFA, with\_SFA and ideal}). \tag{9}$$

In particular, it is easily confirmed that the FRAC signal $S_{\mathrm{SH,ideal}}$ is equivalent to Eq. (1).

Let us introduce the convenient value $\varepsilon_{\alpha,\beta}$ for the evaluation of the difference between FRAC signals $S_{\mathrm{SH},\alpha}(\tau)$s,

RMS (root means square) error $\varepsilon_{\alpha,\beta}$

$$\varepsilon_{\alpha,\beta} \equiv \sqrt{\int_{-\infty}^{\infty} \left(s_\alpha(\tau) - s_\beta(\tau)\right)^2 \mathrm{d}\tau} \;\; (\alpha,\beta = \text{no\_SFA, with\_SFA and ideal}), \tag{10}$$

and the value $r_{\alpha,\beta}$ for the evaluation of the difference between full widths at half-maximum (FWHMs) of their envelopes,

ratio of FWHMs of the envelope $r_{\alpha,\beta}$

$$r_{\alpha,\beta} \equiv \frac{\Delta t_\alpha}{\Delta t_\beta} \;\; (\alpha,\beta = \text{no\_SFA, with\_SFA and ideal}), \tag{11}$$

where

$$s_\alpha(\tau) \equiv \frac{8 S_{\mathrm{SH},\alpha}(\tau)}{S_{\mathrm{SH},\alpha}(0)} \quad (\alpha = \text{no\_SFA, with\_SFA and ideal}) \tag{12}$$

and Δt_α is FWHM of the envelope of $s_\alpha(\tau)$. For Gaussian transform-limited (TL) pulses, we have the well-known value $\Delta t_{\mathrm{ideal}}/t_{\mathrm{p,in}}^{\mathrm{TL}} = 1.7$, where $t_{\mathrm{p,in}}^{\mathrm{TL}}$ is its pulse duration. The envelope function is calculated by absolute values of oscillating terms in $s_\alpha(\tau)$ (corresponding to $F_1(\tau)$ and $F_2(\tau)$ in Eq. [1])].

For example, in the case of α = ideal, the envelope function $S_{\mathrm{env}}(\tau)$ is exactly equivalent to the following equation in the temporal domain [1],

$$S_{\mathrm{env}}(\tau) \quad = \quad 2G(0) + 4G(\tau) + 4|F_1(\tau)| + 2|F_2(\tau)|. \tag{13}$$

3. Numerical analysis: deviation of practical FRAC signal from ideal FRAC signal

Figure 1 shows an example of the difference among three FRAC signals of $s_{\mathrm{ideal}}(\tau)$, $s_{\mathrm{no\_SFA}}(\tau)$, and $s_{\mathrm{with\_SFA}}(\tau)$, where $t_{\mathrm{p,in}}^{\mathrm{TL}}$ =4.01 fs, spectral FWHM $\Delta\nu_{\mathrm{in}} = 110$ THz, the center wavelength $\lambda_{\mathrm{c}} = 600$ nm, the angle between the incident pulse-train beam and the optic axis of 10-μm-thick BBO $\theta = 25^\circ$ (hereafter called the θ crystal angle). The dispersion and related values of n_{o} and n_{e} of type I BBO are taken from Ref. [12]. This case indicates that the apparent pulse duration obtained from the FRAC signal $s_{\mathrm{no\_SFA}}(\tau)$ that considers the bandwidth-limited SH-generation effect without spectral filter approximation is shorter than the correct pulse duration obtained from the FRAC signal $s_{\mathrm{ideal}}(\tau)$, which is not affected by its effect at all.

We investigated in detail estimation values $\varepsilon_{\alpha,\beta}$ and $r_{\alpha,\beta}$ as functions of temporal FWHM $t_{\mathrm{p,in}}^{\mathrm{TL}}$ of Gaussian TL pulses to be measured (the corresponding spectral FWHM $\Delta\nu_{\mathrm{in}}$) and the crystal angle θ for different pulse center wavelengths λ_{c}s (Figs. 2 and 3). In the following numerical calculations, we assumed that the nonlinear crystal for the SH generation is type I 10-μm-thick

#4106 - $15.00 US Received 26 March 2004; revised 14 May 2004; accepted 6 June 2004

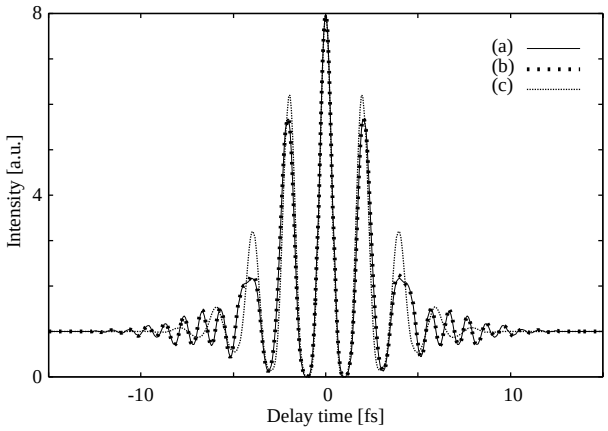

Fig. 1. Calculated FRAC traces for Gaussian TL pulses ($t^{\mathrm{TL}}_{\mathrm{p,in}} = 4.01$ fs, $\Delta\nu_{\mathrm{in}}$, 110 THz; center wavelength, 600 nm; θ=25°; $\varepsilon_{\mathrm{no\_SFA,ideal}}/\varepsilon_{\mathrm{max}} = 0.078$; $\varepsilon_{\mathrm{no\_SFA,with\_SFA}}/\varepsilon_{\mathrm{max}} = 0.0053$; $r_{\mathrm{no\_SFA,ideal}} = 0.88$) (a) with taking account of the bandwidth-limited SH-generation effect without filter approximation [$s_{\mathrm{no\_SFA}}(\tau)$], (b) after filter approximation [$s_{\mathrm{with\_SFA}}(\tau)$] and (c) without the bandwidth limitation effect [$s_{\mathrm{ideal}}(\tau)$].

BBO and limited the Gaussian spectrum to 400–2600 nm in consideration of the fact that the transparency range of BBO is approximately 200–2600 nm (we permitted the Gaussian pulses to have over-one-octave bandwidth). As a result, the following important findings were obtained (Figs. 2–5):

1. The relations $\varepsilon_{\mathrm{no\_SFA,with\_SFA}} \ll \varepsilon_{\mathrm{no\_SFA,ideal}}$ and $|r_{\mathrm{no\_SFA,with\_SFA}} - 1| \ll |r_{\mathrm{no\_SFA,ideal}} - 1|$ are satisfied over the whole $t^{\mathrm{TL}}_{\mathrm{p,in}} - \theta$ region (441 fs $\geq t_{\mathrm{p,in}} \geq$ 2.3 fs; 10° $\leq \theta \leq$ 45°, $\lambda_{\mathrm{c}} = 600$, 700 and, 800 nm; see Fig. 2), and any critical difference between $s_{\mathrm{no\_SFA}}(\tau)$ and $s_{\mathrm{with\_SFA}}(\tau)$ is not found (for example, see Fig. 1). Therefore, it is valid that we interpret results by utilizing the filter function $R(\Omega)$.

2. Note the angle θ_{opt} where the value of $\varepsilon_{\mathrm{no\_SFA,ideal}}$ is minimum ($= \varepsilon^{\mathrm{min}}_{\mathrm{no\_SFA,ideal}}$). For example, $\varepsilon^{\mathrm{min}}_{\mathrm{no\_SFA,ideal}}/\varepsilon_{\mathrm{max}} = 0.155$ at $\theta_{\mathrm{opt}} = 39.2°$, $t^{\mathrm{TL}}_{\mathrm{p,in}} = 5.0$ fs (FRAC ideal's ($= s_{\mathrm{ideal}}(\tau)$'s) FWHM $\Delta t_{\mathrm{ideal}} = 8.51$ fs and $\Delta\nu_{\mathrm{in}} = 88$ THz) and $\lambda_{\mathrm{c}} = 600$ nm, where $\varepsilon_{\mathrm{max}} = 7.083 \times 10^{-15}$ indicated the greatest value of all the calculated $\varepsilon_{\alpha,\beta}$s. This corresponds to the result that $\Delta t_{\mathrm{no\_SFA}} = 8.99$ fs is longer than $\Delta t_{\mathrm{ideal}}$ = 8.51 fs. For λ_{c} = 600, 700, and 800 nm, $\varepsilon_{\mathrm{no_SFA,ideal}}$s become the least ($= \varepsilon^{\mathrm{min}}_{\mathrm{no_SFA,ideal}}$) around θ_{opt} = 39°, 31°, and 24° in the range of $t^{\mathrm{TL}}_{\mathrm{p,in}}$ of 2.3–441 fs, respectively (see dotted lines in Fig. 2). Each angle nearly corresponds to the angle θ_{R} where the wavelength at the maximum value of $R(\Omega)$ equals half of λ_{c} (θ_{R} = 38.5°, 30°, and 22.9° for λ_{c} = 600, 700, and 800 nm, respectively (see Table. 1). It should be noted that these optimal angles θ_{opt}s do not agree with phase-matched angles θ_{pm} of the crystal (θ_{pm} = 40.2°, 33.4°, and 29° for 600, 700, and 800 nm, respectively). In addition, their θ_{opt}s do not agree with the angles θ_{max}s where the strength of the FRAC signal becomes maximum (see Table. 1).

3. The longer λ_{c} is, the smaller $\varepsilon_{\mathrm{no\_SFA,ideal}}$ is. This is because θ_{R} has the smaller value for pulses with longer λ_{c}, and the bandwidth of $R(\Omega)$ with the smaller θ_{R} is the broader (see Fig. 4). That is, pulses with the longer center wavelength are less affected by the filter effect of the nonlinear crystal.

#4106 - $15.00 US Received 26 March 2004; revised 14 May 2004; accepted 6 June 2004

4. The duration ratio $r_{\mathrm{no\_SFA,ideal}}$ at the angle θ_{opt} where $\varepsilon_{\mathrm{no\_SFA,ideal}}$ has the minimum value with respect to $t^{\mathrm{TL}}_{\mathrm{p,in}}$ is shown in Fig. 5. The ratio $r_{\mathrm{no\_SFA,ideal}}$ is always larger than 1 and increases with the decrease of $t^{\mathrm{TL}}_{\mathrm{p,in}}$. That is, the apparent pulse duration at $\theta \simeq \theta_{\mathrm{opt}}$ should be evaluated to be slightly longer than the correct one.

5. Except for the $\theta \simeq \theta_{\mathrm{opt}}$ region, there is the region where $r_{\mathrm{no\_SFA,ideal}}$ is less than 1; that is, the apparent pulse duration should be shorter than the correct one [for example, see the $r_{\alpha,\beta} < 1$ region in Figs. 3(A) and 3(B)].

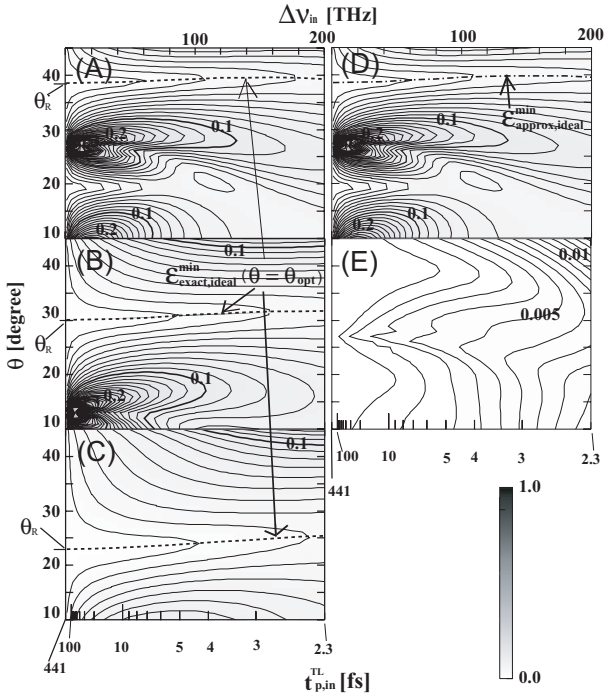

Fig. 2. Contour plots of $\varepsilon_{\alpha,\beta}/\varepsilon_{\mathrm{max}}$ ($\varepsilon_{\mathrm{max}} = 7.083\times10^{-15}$) as functions of the input pulse duration $t^{\mathrm{TL}}_{\mathrm{p,in}}$ and the crystal angle θ. $\varepsilon_{\mathrm{no\_SFA,ideal}}/\varepsilon_{\mathrm{max}}$ at (A) λ_{c} = 600, (B) 700, and (C) 800 nm. (D) $\varepsilon_{\mathrm{with\_SFA,ideal}}/\varepsilon_{\mathrm{max}}$ and (E) $\varepsilon_{\mathrm{no\_SFA,with\_SFA}}/\varepsilon_{\mathrm{max}}$ at λ_{c} = 600 nm.

Table 1. θ_{pm}, θ_{R}, θ_{opt}, θ_{max} for TL Gaussian pulses with $\lambda_{\mathrm{c}} = 600$, 700, and 800 nm (see the text for notation).

			For $t^{\mathrm{TL}}_{\mathrm{p,in}} = 5$ fs pulses		For $t^{\mathrm{TL}}_{\mathrm{p,in}} = 10$ fs pulses	
λ_{c} [nm]	θ_{pm} [deg.]	θ_{R} [deg.]	θ_{opt} [deg.]	θ_{max} [deg.]	θ_{opt} [deg.]	θ_{max} [deg.]
600	40.2	38.5	39.2	40.7	38.7	40.3
700	33.4	30	30.8	33.9	30.2	33.4
800	29	22.9	23.7	29.4	23.1	28.8

#4106 - $15.00 US
Received 26 March 2004; revised 14 May 2004; accepted 6 June 2004

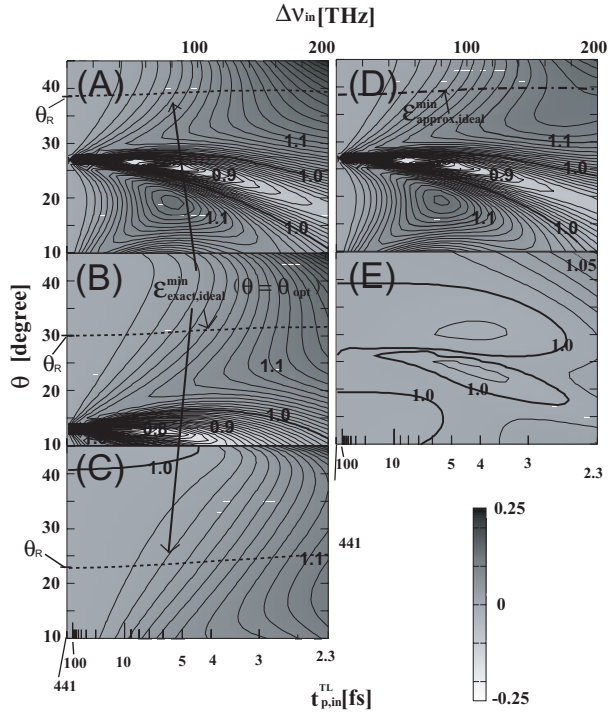

Fig. 3. Contour plots of $r_{\alpha,\beta}$ as functions of the input pulse duration $t_{\mathrm{p,in}}^{\mathrm{TL}}$ and the crystal angle θ. $r_{\mathrm{no\_SFA,ideal}}$ at (A) λ_{c} = 600, (B) 700, and (C) 800 nm. (D) $r_{\mathrm{with\_SFA,ideal}}$ and (E) $r_{\mathrm{no\_SFA,with\_SFA}}$ at λ_{c} = 600 nm.

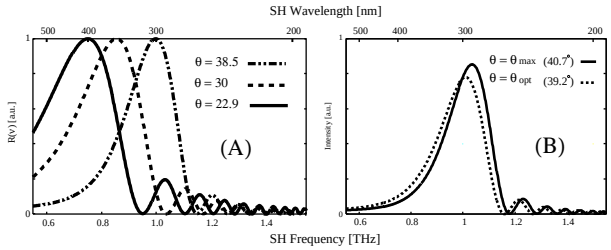

Fig. 4. Plots of the SH frequency-dependent filter function $R(\Omega)$ of (A) normalized ones and (B) nonnormalized ones at various values of crystal angle θ.

4. Experiments

We carried out few-cycle-pulse experiments for verification of the above-mentioned filter effect. Our experimental setup was almost the same as in Ref. [8]. Optical pulses from a Ti:sapphire laser amplifier system (repetition rate, 1 kHz; center wavelength, 790 nm; pulse duration, $<$30 fs; pulse energy, $\sim$200 μJ/pulse) were broadened by self-phase modulation (SPM) in an Ar-filled hollow fiber and then guided into a feedback chirp compensation system [8] that consists of a modified-SPIDER (M-SPIDER) apparatus with a high sensitivity [7] and a 4-f phase compensator with a liquid-crystal spatial light modulator [2]. The bandwidth of the spec-

#4106 - $15.00 US
Received 26 March 2004; revised 14 May 2004; accepted 6 June 2004

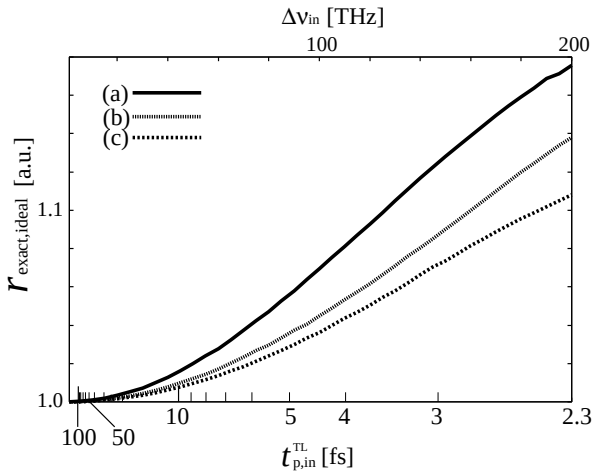

Fig. 5. Plots of $r_{\mathrm{no\_SFA,ideal}}$ at $\varepsilon = \varepsilon^{\mathrm{min}}_{\mathrm{no\_SFA,ideal}}$ for the input pulse duration $t^{\mathrm{TL}}_{\mathrm{p,in}}(\Delta\nu_{\mathrm{in}})$. Each plot for (a) λ_{c}, 600 nm; (b) λ_{c}, 700 nm; and (c) λ_{c}, 800 nm.

trum was limited to 530–980 nm by use of a slit in the 4-f phase compensator, to avoid the background-light noise resulting from fundamental pulses in FRAC measurements. We used a reflective dielectric filter with a nearly flat reflectance over approximately 250–500 nm (cutoff 500 nm) to separate the SH signal from fundamental pulses. It had been confirmed that a spectral sensitivity of a photodiode for detection of the SH signal does not give the practical change to FRAC traces by numerical calculation in our present case. The chirp of the fiber output pulses was almost completely compensated for by this feedback system, and then compensated pulses were independently measured by the FRAC apparatus with 10-μm-thick BBO (type I, θ=29°). To compare FRAC and M-SPIDER measurements precisely, we aligned those apparatuses to equalize optical path lengths to nonlinear crystals and used beams splitters with the same properties (thickness, 0.5 mm; substrate, fused-silica; 20% reflection and 80% transmission for s polarization from 400 to 1300 nm) for symmetric Michelson interferometers [10] in both apparatuses.

To clarify the practical limitation of the FRAC method, experiments for two cases (cases M-1 and M-2) were performed.

- Case M-1: 5.3-fs ($t_{\mathrm{p,in}}$), 2.2-cycle pulses with a center wavelength of 725.1 nm (λ_{c}) and a TL pulse duration of 4.42 fs ($t^{\mathrm{TL}}_{\mathrm{p,in}}$) [Figs. 7(A) and 7(B)]. An Ar pressure of $p = 1.0$ atm.
- Case M-2: 3.6-fs ($t_{\mathrm{p,in}}$), 1.7-cycle pulses with a wavelength of 617.5 nm (λ_{c}) and a TL pulse duration of 3.5 fs ($t^{\mathrm{TL}}_{\mathrm{p,in}}$) [Figs. 8(A) and 8(B)]. An Ar pressure of $p = 3.0$ atm.

The center wavelength λ_{c} was calculated by an equation
$2\pi c/\lambda_{\mathrm{c}} = \int_{-\infty}^{\infty} \omega|\tilde{E}(\omega)|^2 \mathrm{d}\omega / \int_{-\infty}^{\infty} |\tilde{E}(\omega)|^2 \mathrm{d}\omega$.

4.1. Comparison between TL-pulse FRAC signals based on measured and corresponding Gaussian spectra

First of all, we calculated and compared FRAC traces of TL pulses using two measured spectral cases M-1 and M-2 and those using corresponding Gaussian spectral cases G-1 and G-2. We discussed them using the same pulse duration $t^{\mathrm{TL}}_{\mathrm{p,in}}$ and center wavelength λ_{c}.

#4106 - $15.00 US Received 26 March 2004; revised 14 May 2004; accepted 6 June 2004

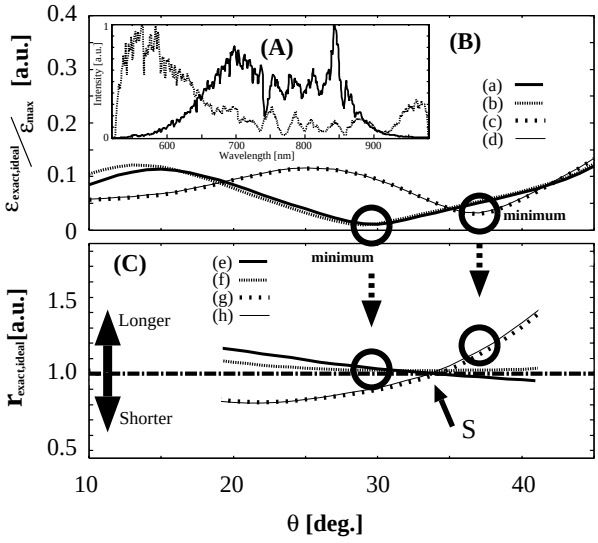

Fig. 6. (A) Measured spectra at the pressure p = 1.0 and 3.0 atm. (B) Dependency of $\varepsilon_{\mathrm{no\_SFA,ideal}}$ on the crystal angle θ for (a) TL pulse at p = 1.0 atm, (b) retrieved one by M-SPIDER measurement at p = 1.0 atm, (c) TL pulse at p = 3.0 atm, and (d) retrieved one by M-SPIDER measurement at p = 3.0 atm. (C) Dependency of $r_{\mathrm{no\_SFA,ideal}}$ on the crystal angle θ for (e) TL pulse at p = 1.0 atm, (f) retrieved one by M-SPIDER measurement at p = 1.0 atm, (g) TL pulse at p = 3.0 atm, and (h) retrieved one by M-SPIDER measurement at p = 3.0 atm.

It was confirmed that the θ_{opt} between cases M-i and G-i ($i = 1$ and 2) has almost the same value as well as θ_{max} (see Table 2) and $\theta_{\mathrm{opt}} \simeq \theta_{\mathrm{R}}$, but $\varepsilon^{\mathrm{min}}_{\mathrm{no\_SFA,ideal}}$ and $r_{\mathrm{no\_SFA,ideal}}$ have different values in the different cases. However, for $\sim$10-fs TL pulses θ_{opt}, $\varepsilon^{\mathrm{min}}_{\mathrm{no\_SFA,ideal}}$, and $r_{\mathrm{no\_SFA,ideal}}$ for measured and Gaussian spectral cases were not different. In addition, the filter effect of the nonlinear crystal hardly caused evaluation errors for $\sim$10-fs pulse durations.

Figures 6(B) and 6(C) show dependencies of the normalized $\varepsilon_{\mathrm{no\_SFA,ideal}}$ and the $r_{\mathrm{no\_SFA,ideal}}$ on the crystal angle θ for cases M-1 and M-2. Those figures indicate that the θ_{opt}s for cases M-1 and M-2 are 29.7° and 36.8°, where both measured apparent pulse durations become slightly longer than correct pulse durations. Around $\theta = 34°$ [around S in Fig. 6(C)], $r_{\mathrm{no_SFA,ideal}}$s are $\sim$1, although $\varepsilon_{\mathrm{no_SFA,ideal}}$s do not have the minimum values. However, we should not measure the FRAC trace around such region of $\theta \sim 34°$. This is because the FRAC signal is often distorted so remarkably, except at $\theta \sim \theta_{\mathrm{opt}}$, that the spacing of the fringe differs, especially in its both wings, from that at $\theta \sim \theta_{\mathrm{opt}}$, even though the apparent FRAC-envelope ratio $r_{\mathrm{no\_SFA,ideal}}$ becomes $\sim$1.

Moreover, we find that when pulse durations are measured around $\theta \simeq 40°$ for case M-1 and around $\theta \simeq 20°$ for case M-2, both apparent durations become shorter than correct pulse durations, as previously reported [2, 3, 4, 5].

4.2. Experimental comparison between directly measured and M-SPIDER-retrieved FRAC signals

We compared measured FRAC traces with traces retrieved from M-SPIDER measurements [7, 8] for cases M-1 and M-2. Experimental results are shown in Fig. 7(C) for M-1 and Fig. 8(C)

#4106 - $15.00 US
Received 26 March 2004; revised 14 May 2004; accepted 6 June 2004

for M-2. Curves (a), (b), and (c) of (A) in those Figs. 7 and 8 show the intensity spectrum ($\propto |\tilde{E}(\omega)|^2$), the spectral phase before chirp compensation, and the spectral phase [$\phi(\omega)$] after compensation, respectively. Curves (d), (e), and (f) of (B) show the temporal intensity [$I(t)$], the temporal phase [$\varphi(t)$], and the TL pulse profile, respectively. Curves (i) of (C) show FRAC traces measured at the angle $\theta = 29^\circ$ (close to the $\theta_{\rm opt}$ for case M-1; see Table. 2) of 10-μm thick BBO, and curves (ii) and (iii) of (C) show FRAC traces retrieved from $s_{\rm no\_SFA}(\tau)$ and $s_{\rm ideal}(\tau)$ in Eq. (12) using M-SPIDER results of $\phi(\omega)$ and $|\tilde{E}(\omega)|$, respectively.

In case M-1 ($t_{\rm p,in} = 5.3$ fs, 2.2 cycles, $t_{\rm p,in}^{\rm TL} = 4.42$ fs, and $\lambda_{\rm c} = 725.1$ nm), we could not find explicit differences among curves (i)–(iii), as expected from calculated results of Figs. 6(B) and 6(C) [curves (b) and (f)]. On the other hand, in case M-2 ($t_{\rm p,in} = 3.6$ fs, 1.7 cycles, $t_{\rm p,in}^{\rm TL} = 3.50$ fs, and $\lambda_{\rm c}$ =617.5 nm), the measured FRAC trace [curve (i)] agrees with the retrieved trace [curve (ii)] with taking account of the bandwidth-limited SH-generation effect without spectral filter approximation, but there is the unignorable difference between curves (i) and (iii) (the retrieved trace without the spectral filter effect), as expected from calculated results of Figs. 6(B) and 6(C) [curves (d) and (h)]. Therefore, it was verified that the FRAC trace of pulses shorter than sub-5 fs was seriously distorted by the spectral filter effect because of the nonlinear crystal. In addition, in comparing curves (ii) and (iii) in Fig. 8(C), we found that $\Delta t_{\rm no\_SFA}$ is 11% smaller than $\Delta t_{\rm ideal}$. That is to say, the apparent pulse duration may be evaluated to be 3.16 fs. This implies that the apparent pulse duration evaluated by the FRAC measurement is shorter than that of the TL pulse. This result agrees with not only the calculated result of Fig. 6 but also previously reported results [2, 3, 4, 5].

When the deviation of $r_{\rm no\_SFA,ideal}$ from 1 is less than $\sim$5% at $\theta \sim \theta_{\rm opt}$, we could not recognize any practical difference in the FRAC traces between $s_{\rm no\_SFA}(\tau)$ and $s_{\rm ideal}(\tau)$ for all the FRAC traces calculated in this paper. Therefore, we can assume that such FRAC traces are not nearly distorted, and it is not necessary to take account of the bandwidth-limitation effect. In fact, in accumulative measurements of one FRAC trace of usual, repetitive pulses, a $\sim$5% margin of the error is assumed to be reasonable when one considers the actual FRAC trace noise, the fluctuation of the pulse intensity, and the delay time error.

5. Conclusion

The practical limitation of the FRAC method with 10-μm-thick BBO for characterization of few-optical-cycle pulses with center wavelengths of 600–800 nm was demonstrated experimentally and theoretically. For TL pulses longer than sub-5 fs, the FRAC measurement under the suitable crystal angle is consistently available. On the other hand, for TL pulses shorter than sub-5 fs, the FRAC measurement even under the suitable crystal angle does not provide the correct result, because of the spectral filter $R(\Omega)$ effect of the nonlinear crystal. However, numerical consideration and correction of this $R(\Omega)$ effect greatly reduce the evaluation errors of FRAC measurements and improve reliability of their measurement results.

Acknowledgments

We are grateful to Akira Sugro (Citizen Co. Ltd.) for supplying a specially designed liquid-crystal SLM.

Table 2. θ_{pm}, θ_R, θ_{opt}, and θ_{max} for Gaussian spectrum (G-i) and measured spectrum (M-i) ($i = 1$, $t_{p,in}^{TL} = 4.42$ fs $\lambda_c = 725.1$ nm; $i = 2$, $t_{p,in}^{TL} = 3.5$ fs $\lambda_c = 617.5$ nm (see text for notation[a]).

	θ_{pm} [deg.]	θ_R [deg.]	θ_{opt} [deg.]	θ_{max} [deg.]	λ_c [nm]
M-1	32.2	28.1	29.7 (PH, 28.9)	33.3 (PH, 32.5)	725.1
G-1	32.2	28.1	29.1	32.8	725.1
M-2	38.8	36.9	36.8 (PH, 36.7)	39.4 (PH, 39.5)	617.5
G-2	38.8	36.9	37.9	39.7	617.5

[a]In all the cases except for the case of "PH" where spectral phases measured by M-SPIDER were also used, θ_{opt}s and θ_{max}s were calculated by use of their transform-limited pulses.

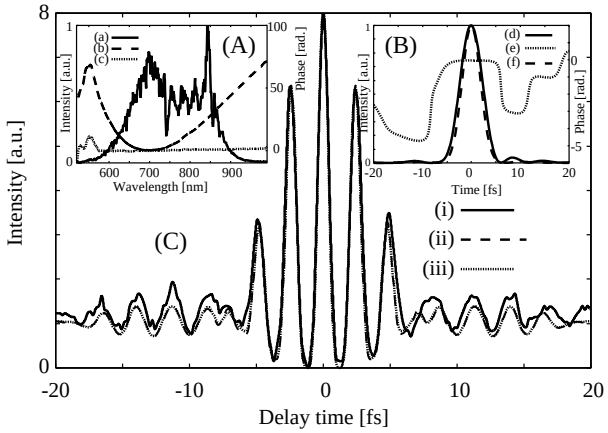

Fig. 7. Experimental results (Ar-gas pressure, 1.0 atm; fiber input, 150 μJ/pulse; fiber output, 16.5 μJ/pulse). (A) (a) Intensity spectrum and spectral phases (b) before and (c) after feedback chirp compensation. (B) (d) Temporal intensity (pulse duration: 5.3 fs, center wavelength: 725.1 nm) and (e) temporal phase after chirp compensation. (f) Temporal intensity of the Fourier transform-limited pulse (pulse duration: 4.42 fs). (C) (i) Measured FRAC trace and retrieved FRAC traces (ii) with and (iii) without taking account of the filter effect by the nonlinear crystal.

#4106 - $15.00 US Received 26 March 2004; revised 14 May 2004; accepted 6 June 2004

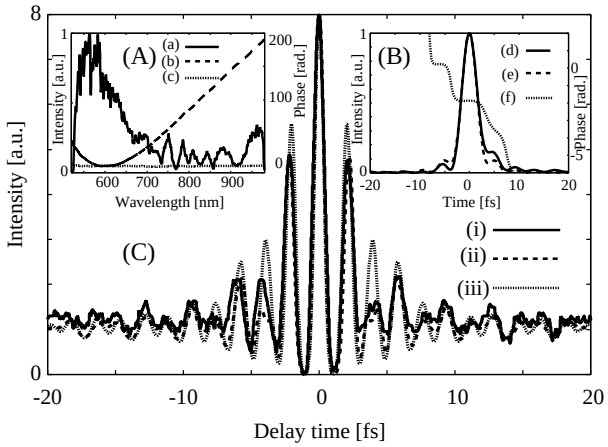

Fig. 8. Experimental results (Ar-gas pressure: 3.0 atm, fiber input: 140 μJ/pulse, fiber output: 18 μJ/pulse). (A) (a) Intensity spectrum and spectral phases (b) before and (c) after feedback chirp compensation. (B) (d) Temporal intensity (3.6 fs, center wavelength: 617.5 nm) and (e) temporal phase after chirp compensation. (f) Temporal intensity of the Fourier transform-limited pulse (3.50 fs). (C) (i) Measured FRAC trace and retrieved FRAC traces (ii) with and (iii) without taking account of the filter effect by the nonlinear crystal.

#4106 - $15.00 US
Received 26 March 2004; revised 14 May 2004; accepted 6 June 2004